Energetics of DNA Intercalation Reactions†

Jinsong Ren,‡ Terence C. Jenkins,*,§ and Jonathan B. Chaires*,‡

Department of Biochemistry, University of Mississippi Medical Center, 2500 North State Street, Jackson, Mississippi 39216-4505, and YCR Laboratory of Drug Design, Cancer Research Group, Department of Biomedical Sciences, University of Bradford, Bradford, West Yorkshire BD7 1DP, U.K.

Received March 1, 2000; Revised Manuscript Received May 2, 2000

ABSTRACT: Isothermal titration calorimetry has been used to determine the binding enthalpy and heat capacity change (ΔC_p) for a series of DNA intercalators, including ethidium, propidium, daunorubicin, and adriamycin. Temperature-dependent binding enthalpies were measured directly for the ligands, from which ΔC_p values of −140 to −160 cal mol^{-1} K^{-1} were calculated. Published van't Hoff plots were reanalyzed to obtain ΔC_p values of −337 to −423 cal mol^{-1} K^{-1} for the binding of actinomycin D to several DNA oligonucleotide duplexes with defined sequences. Heat capacity changes for DNA intercalation were found to correlate with the alterations in solvent-accessible surface area calculated from available high-resolution structural data. Multiple linear regression was used to derive the relationship $\Delta C_p = 0.382(\pm 0.026)\Delta A_{np} - 0.121(\pm 0.077)\Delta A_p$ cal mol^{-1} K^{-1}, where ΔA_{np} and ΔA_p are the binding-induced changes in nonpolar and polar solvent-accessible surface areas (in square angstroms), respectively. The ΔC_p terms were used to estimate the hydrophobic contribution to intercalative binding free energies, yielding values that ranged from −11.2 (ethidium) to −30 kcal mol^{-1} (actinomycin D). An attempt was made to parse the observed binding free energies of ethidium and propidium into five underlying contributions. Such analysis showed that the DNA binding behavior of these simple intercalators is driven almost equally by hydrophobic effects and van der Waals contacts within the intercalation site.

The rational design of new DNA binding agents that bind selectively to specific sequences or structures is an area of great interest and urgency (*1*−*4*). Small synthetic molecules that target a particular DNA site might be used to selectively inhibit or modulate gene expression, and would be valuable for a variety of chemotherapeutic strategies (*2*−*5*). The design process for such agents has largely been dominated by structure-based principles for the past two decades. However, while structural studies clearly provide an important departure point for this exercise, the integration of energetic factors into the design process could yield an even more powerful strategy (*6*, *7*). Energetic data provide an inherently superior basis for defining the molecular forces that drive a particular binding reaction and, importantly, offer a means for understanding in quantitative detail the contributions of specific ligand substituents to the recognition and binding events (*8*). Unfortunately, detailed thermodynamic studies of DNA−drug interactions have been comparatively sparse, hampering efforts to build a reliable database for use in integrating energetic considerations into the overall design process. Measurements of DNA−drug binding constants (readily converted to standard binding free energy changes, $\Delta G°$) are relatively common (*9*), but determinations of reliable binding enthalpies ($\Delta H°$) and entropies ($\Delta S°$) are not (*6*). Even more sparse are determinations of heat capacity changes [$\Delta C_p = \delta(\Delta H°)/\delta T$] for DNA−drug binding.

Sturtevant first called attention to the importance of heat capacity changes in reactions involving biopolymers (*10*). Enormous effort from several laboratories, stimulated by the advent of modern microcalorimeters, subsequently resulted in the accurate determination of $\Delta H°$ and ΔC_p values for a number of protein denaturation and binding reactions (reviewed in refs *11* and *12*), and for several DNA−protein interactions (*13*). Precise ΔC_p values are particularly valuable for understanding binding reactions for at least two reasons. First, empirical relationships were derived that correlate ΔC_p values with changes in solvent-accessible surface areas (SASAs)[1] that accompany a reaction, providing a direct link between thermodynamic and structural data (*13*). Second, ΔC_p values can be used to quantitatively estimate the contribution of hydrophobic interactions to the free energy of a binding reaction (*13*), making it possible to begin to parse the free energies and hence to evaluate the relative importance of component intermolecular terms.

We recently reported a detailed thermodynamic study of the interaction of the minor groove binder Hoechst 33258 to an oligonucleotide duplex containing a single ligand binding site (*7*). An accurate ΔC_p value was obtained and found to correlate well with the binding-induced alteration in SASA, as computed from crystal structures determined for the DNA−dye complex. One striking conclusion to

† This work was supported by the National Cancer Institute (Grant CA35635 to J.B.C.) and Yorkshire Cancer Research of the U.K. (program grant to T.C.J.).

* To whom correspondence should be addressed. J.B.C.: phone, (601) 984-1523; fax, (601) 984-1501; e-mail, jchaires@biochem.umsmed.edu. T.C.J.: phone, (+044) 1274-236480; fax, (+044) 1274-233234; e-mail, t.c.jenkins@brad.ac.uk.

‡ University of Mississippi Medical Center.

§ University of Bradford.

[1] Abbreviations: ITC, isothermal titration calorimetry; SASA, solvent-accessible surface area.

10.1021/bi000474a CCC: $19.00
Published on Web 06/27/2000

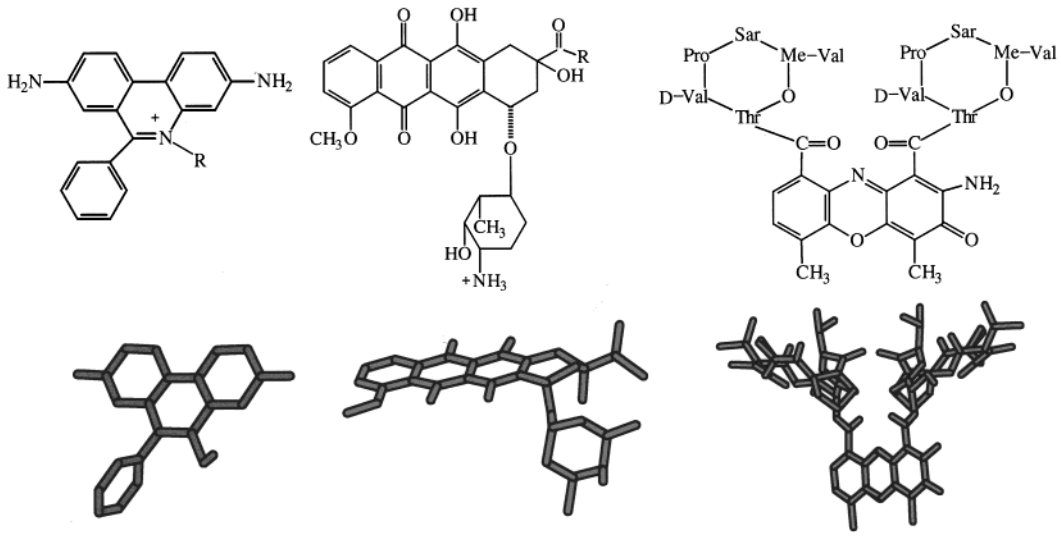

FIGURE 1: (Top) Structures of the intercalators used in this study. (Left) Ethidium (R = CH_2CH_3) and propidium [R = $(CH_2)_3N^+MeEt_2$]. (Center) Daunorubicin (R = CH_3) and adriamycin (R = CH_2OH). (Right) Actinomycin D. (Bottom) The energy-minimized molecular profiles for ethidium, daunorubicin, and actinomycin D illustrate the different chromophores that are involved.

emerge from this study was that the overwhelming driving force for binding stems from hydrophobic effects, and that H-bonded interactions contribute comparatively little if anything to the stabilization of the groove-bound complex. This conclusion stands in sharp contrast to the viewpoint of many structural biologists, where attention has focused on hydrogen bonding as a key factor in dictating stability for DNA minor groove ligands (e.g., ref *14*). While such H-bonding probably plays a role in modulating the sequence recognition properties of groove-mediated agents, our thermodynamic data clearly imply that other forces drive the binding reaction and contribute the bulk of the favorable binding free energy (*7*).

While there are several reliable calorimetric studies of DNA intercalation reactions that provide binding enthalpies, there a few reported determinations of any ΔC_p values (*6*). Hopkins and co-workers reported ΔC_p values of 10 and -57 cal mol^{-1} K^{-1} for the intercalation of ethidium and propidium, respectively, into double-stranded calf thymus DNA (*15*). Relative errors of 5% were claimed for these values. More recently, a ΔC_p value of $-75(\pm 38)$ cal mol^{-1} K^{-1} was reported for ethidium binding to chromatin (*16*). While numerous studies have reported enthalpy values for intercalation reactions based on the temperature dependence of binding constants and van't Hoff analysis, a recent study (*17*) showed that reliable ΔC_p values are difficult to obtain by that approach unless they are large in magnitude (i.e., $>|200|$ cal mol^{-1} K^{-1}).

The primary goal of our study was to obtain reliable heat capacity changes for the binding of representative intercalators to duplex-form DNA by using isothermal titration calorimetry (ITC). The enthalpies of binding of ethidium, propidium, daunorubicin, and adriamycin (Figure 1) to calf thymus DNA were studied as a function of temperature. Binding ΔC_p values were next obtained and correlated with the changes in solvent-accessible surface area (SASA) computed from structures deposited for the intercalated DNA complexes with these compounds.

MATERIALS AND METHODS

Materials. All experiments were carried out in aqueous salt-supplemented BPE-S buffer (*18*) at pH 7.00 ± 0.01 (6 mM Na_2HPO_4, 2 mM NaH_2PO_4, 1 mM EDTA, and 185 mM NaCl). Ethidium bromide, propidium iodide, daunorubicin (daunorubicin, NSC-82151), and adriamycin (doxorubicin, NSC-123127) were purchased from Sigma Chemical Co. (St. Louis, MO) and used without further purification. Solution concentrations of ethidium and propidium were determined by visible spectrophotometry at 480 and 493 nm using molar extinction coefficients ϵ_{480} and ϵ_{493} of 5600 and 5800 M^{-1} cm^{-1}, respectively. Buffered solutions of daunorubicin and adriamycin were similarly quantitated at 480 nm assuming $\epsilon_{480} = 11\,500$ M^{-1} cm^{-1}. Calf thymus DNA (CT-DNA) was purchased from Pharmacia (lot no. 274562-02), and was sonicated and purified as described previously (*19*). Before further use, the DNA was dialyzed in BPE-S buffer for 24 h.

Isothermal Titration Calorimetry (ITC). Calorimetric data were obtained using a Calorimetric Sciences Corp. (Provo, UT) isothermal microtitration calorimeter linked to a Gateway 2000 personal computer. The reference cell was filled with distilled water. The instrument was routinely calibrated using the neutralization of NaOH by HCl as a calibration reaction, where an enthalpy value of 13.63 kcal mol^{-1} at 20 °C has been accurately determined (*20*). Both reagents are available as highly pure, standardized aqueous solutions from Aldrich Chemical Co. (St. Louis, MO). For instrument calibration (*21*, *22*), a 0.0995 M NaOH volumetric solution (cell volume of 1.00 mL) was titrated with serial 3 μL injections of an aqueous 0.1036 M HCl solution. Data for up to 20 injections in a single run were accumulated and averaged for comparison with the known enthalpy value.

Binding enthalpies for the intercalator ligands were determined using the "model-free ITC" protocol to obtain multiple estimates of $\Delta H°$ and to avoid any possible fitting bias (*22*). In this procedure, a large excess of DNA is placed in the calorimeter cell and aliquots of the ligand are then titrated into the DNA solution following thermal equilibration. The high DNA concentration ensures that all added

ligand is effectively bound after each serial addition. Integration of each titration peak and normalization for the number of moles of ligand added provides a direct and model-free estimate of the binding enthalpy, without recourse to any curve fitting or assumed binding model(s). Specifically, 1 mL of a 1 mM (in bp) CT-DNA solution was loaded into the reaction cell. A stock solution of intercalator (typically 1 mM in BPE-S buffer) was titrated into the DNA solution, usually making 20 injections of 3 μL with 5 min between injections to ensure equilibration. The titrate DNA solution was stirred continuously at 50 rpm over the course of the experiment. Data were collected as heat released (microjoules) in the exothermic reactions versus time (second). The heat of reaction (ΔH) was obtained by integration of the peak obtained after each injection. Heats of dilution for each intercalator were separately determined by injecting ligand solution into the same reaction cell loaded with BPE-S buffer alone. The dilution heats were subtracted from the ΔH value determined for titration into DNA to give a corrected value for the binding-induced enthalpy change. Each titration was carried out at four fixed temperatures between 20 and 45 °C. Attempts to work below 20 °C were hampered by the high ambient humidity in Mississippi. Even with dry gas purging of the instrument, the quality of data obtained at temperatures below 20 °C was not as good as that obtained at and above room temperature. All titration series were repeated at least three times, and the averaged binding enthalpies ($\Delta H°$) were obtained after normalization and necessary correction for any heats of dilution.

The comparatively high concentrations of intercalator needed for ITC titration experiments required us to consider possible effects of drug self-association, which could contribute substantial heats to the apparent heats of dilution. For ethidium, dimerization constants of 30 (*37*) and 270 M^{-1} (*38*) were reported in pure water and 1 M NaCl, respectively. Interpolation to 0.2 M NaCl yields a dimerization constant of 77 M^{-1} under the conditions used in our experiments. That value may be used to determine that at most 6% of our stock ethidium used for titrations was dimerized. Dissolution of that amount of dimer would contribute at most 0.9 μcal to the apparent heat of dilution, assuming a dimerization enthalpy of −5 kcal/mol (*38*). Since the minimum detectable heat of the Calorimetric Sciences ITC is 0.5 μcal, aggregation of ethidium would contribute neglible heat effects. In fact, we found negligible heats of dilution for ethidium and propidium under the conditions used in our experiments. Daunorubicin, in contrast, avidly self-associates (*39*). Using the published self-association constant and enthalpy (*39*), we determine that 73% of the daunorubicin in the stock solution is aggregated, and that dissociation of the aggregate would contribute approximately 17 μcal to the apparent heat of dilution. The measured heat of daunorubicin dilution in the limit as the daunorubicin concentration went to zero was 3.0 kcal/mol in our experiments, which was used to correct the measured binding enthalpy values. There are some additional subtleties in this case. Heats of dilution for the titration of daunorubicin into buffer are not constant, which in fact is a manifestation of the self-association of the drug as concentration increases over the course of the titration. A distinct advantage of the model-free ITC approach, however, is that by design all added drug is bound. The appropriate apparent heat of dilution to use to correct binding data is therefore that measured in the limit of the low drug concentration, as was done. In protocols in which binding sites are saturated, drug self-association would present a daunting difficulty, since at each point in the titration observed heats would need to be corrected for the ever-changing fraction of drug aggregate in the solution, and the correction to be applied would not be constant. Our protocol avoids this difficulty.

Calculation of Solvent-Accessible Surface Areas (SASAs). Accessible surface areas were determined for reported DNA/RNA−intercalator complexes and the DNA and ligand reactants as described previously (*7*, *22*). Briefly, the method exploits the analytical method in the versatile GRASP 1.3.6 program (*23*), where all-atom structures are mapped at high resolution using Lennard-Jones atomic radii and a spherical surface probe with a 1.4 Å radius. Surfaces for carbon, carbon-bound hydrogen, and phosphorus atoms are classified as nonpolar, and those for the remaining hydrophilic atoms are defined as polar. Surfaces were generated from coordinates for X-ray crystallographic or solution NMR structures of the intercalated complexes available from the Nucleic Acid Database (NDB, ndbserver.rutgers.edu) (*24*) or the Brookhaven Protein Data Bank (PDB, www.pdb.bnl.gov). Structures for the free ligands were taken from either the Chemical Database Service (CSSR entry cds1.dl.ac.uk), where available, or by averaging coordinates isolated from the reported DNA−ligand complexes. These geometries showed no significant difference in either geometry or SASA from energy-minimized molecular models. All hydrogen atoms required for each structure were added using standard bond lengths and angles. Structural information is unavailable for any native DNA duplex used to generate the reported intercalator complexes; hence, these structures were constructed using the GENHELIX-2 program (T. C. Jenkins, unpublished) for B-DNA conformations with standard nucleic acid parameters (*24*) and each strand terminated with 5′- or 3′-OH groups.

No structural data are reported for nucleic acid−propidium complexes; hence, structures were generated from the analogous ethidium complexes by side chain construction of the smaller ligand using the NEMESIS 2.0 modeling program (Oxford Molecular Ltd., Oxford, U.K.). Further details are included in the Supporting Information. Relevant charged states were adopted for each ligand (cf. Figure 1) under the buffer solution conditions that were used: ethidium (+1), propidium (+2), daunorubicin (+1), adriamycin (+1), and actinomycin D (no charge).

The change in solvent-accessible molecular surface area on binding, ΔA_{total}, is the difference between the area of the complex and the summed surface areas for the uncomplexed native duplex and unbound ligand reactants:

$$A_{total} = A_{np} + A_p; \qquad \Delta A_{total} = \Delta A_{np} + \Delta A_p$$

where A_{np} and A_p represent surface contributions from nonpolar and polar atoms, respectively. The binding-induced alterations in component SASA terms on forming a DNA−ligand complex with overall 1:*m* stoichiometry are thus given by

$$\Delta A_{np} = A_{np}(1{:}m \text{ complex}) - [A_{np}(\text{native DNA}) + mA_{np} \text{ (free ligand)}]$$

$$\Delta A_{p} = A_{p}(1{:}m \text{ complex}) - [A_{p}(\text{native DNA}) + mA_{p} \text{ (free ligand)}]$$

Full details of the SASA calculations and the effects of DNA binding upon nonpolar and polar reactant surfaces are collected in the Supporting Information for the five intercalator ligands that were examined. For illustration, a SASA intermolecular interface obtained using this procedure is shown in Figure 2 for a 1:1 d(GAAGCTTC)$_2$−actinomycin D complex (*25*), and serves to highlight the effective removal or burial of accessible surfaces from each reactant on intercalative DNA binding.

RESULTS

Figure 3 shows representative primary data from a titration of ethidium into a calf thymus DNA solution at 35 °C using the model-free ITC protocol. The data shown are uncorrected in any way, with no applied smoothing or baseline correction. A signal-to-noise ratio of >100 characterizes the titration data that are shown. Integration of the peaks followed by normalization for the number of moles of added ethidium provides a direct estimate of the binding enthalpy.

Figure 4 shows distributions of binding enthalpy estimates obtained for ethidium at several temperatures in the 20−45 °C range. A total of 60 enthalpy estimates were obtained at each temperature and then averaged. Table 1 shows the mean enthalpy values and estimates of their standard deviations for each of the intercalators that was studied. The temperature-dependent behavior of the enthalpy values (Figure 5) allows heat capacity changes (ΔC_p) to be determined from the slopes of least-squares lines fit to the data. The ΔC_p estimates that are obtained are collected in the last column of Table 1, where the associated ΔC_p error estimates were evaluated by rigorous Monte Carlo methods (*26*). This approach provides, in our opinion, more honest and reliable error estimates than those obtained by using conventional linear least-squares fitting packages. The error in ΔC_p estimates is about 20% in all cases which, given the small magnitudes of the heat capacity changes involved, is probably about as well as one can do with current instrumentation. Measured enthalpy and heat capacity changes represent values averaged for ligand intercalation to heterogeneous sites along the DNA lattice. The distributions shown in Figure 4, which are essentially Gaussian in all cases, represent only the experimental error in the enthalpy measurements and do not reflect site heterogeneity.

Heat capacity changes were obtained for the binding of actinomycin D to defined-sequence oligodeoxynucleotides by reanalysis of van't Hoff plots published by Bailey and Graves (*27*), who reported temperature-independent enthalpy values obtained from linear fits to their experimental data. Closer inspection of their data reveals that the van't Hoff plots are in fact nonlinear in accord with a non-zero value for the ΔC_p parameter. Details of the analytical procedure are provided in the Supporting Information, and the results of our reanalysis of the DNA−actinomycin D system are collected in Table 2.

Changes in the solvent-accessible surface areas upon intercalative complexation with duplex DNA were calculated as described for each of the five ligands examined in this study. Table 3 shows averaged values for the binding-induced changes in nonpolar (ΔA_{np}) and polar (ΔA_p) surface areas for the reported DNA−intercalator systems relative to the DNA duplex and ligand reactants. These values are averages from several different structures that are available from the structural databases, for DNA sequences of various complexion and either 1:1 or 1:2 DNA−ligand binding stoichiometries. No selection was made on the basis of preferred or favored binding sequence for any particular ligand.

Figure 6 shows the correlation between experimental ΔC_p values and changes in nonpolar SASA contribution for each intercalator compound. Also shown (Figure 6) are data tabulated by Livingstone and co-workers (*28*) for a variety of protein unfolding and binding reactions, and for solvent transfer of small hydrocarbons. These data were used to establish the empirical correlation between heat capacity changes and binding-induced surface removal (see below). Our new data reported for the DNA-intercalating ligands fill the previous significant void that separated data obtained for the small-molecule hydrocarbons and the protein systems. It is clear that DNA intercalation reactions evidently follow the general correlation that links changes in heat capacity and nonpolar solvent-accessible molecular surface area.

DISCUSSION

An understanding of DNA intercalation reactions requires a detailed characterization of the thermodynamics of the binding process, together with reliable determinations of both binding enthalpies and heat capacity changes (*6*, *7*, *22*). We now report results from ITC experiments that provide estimates of ΔC_p that are as accurate as possible for a series of DNA intercalants of differing chemical nature. However, as the ΔC_p values for intercalation reactions are only relatively small in magnitude, their accurate determination is difficult and demanding. Table 1 summarizes the data we have obtained.

Reports of ΔC_p estimates for intercalation reactions are sparse and often disagree where reported (*15*, *16*). This disagreement perhaps reflects the practical difficulties associated with the experimental measurements. Previous reports of ΔC_p for ethidium binding to DNA, for example, range from 10 to −75 cal mol^{-1} K^{-1} (*15*, *16*). In contrast, the −139(±30) cal mol^{-1} K^{-1} value we determine here is larger in magnitude than either previous estimate. A reevaluation of the ethidium binding data from two further published reports (*29*, *30*) supports our experimental value, as detailed in the Supporting Information. Briefly, a reanalysis of the curved van't Hoff plot published by Baldini and Varani (*29*) yields a ΔC_p value of −126(±35) cal mol^{-1} K^{-1} that is well within the error of our more direct determination. Further, Sauer and co-workers (*30*) reported enthalpy values obtained for identical solution conditions both by van't Hoff analysis of binding data and by batch calorimetry. The van't Hoff enthalpy estimate was ≈10% higher than the value obtained by calorimetry, a finding consistent with the existence of a small heat capacity change whose contribution to curvature in the van't Hoff plot is hidden within experimental noise but which can bias the slope of the fit used to obtain the enthalpy (*17*). Reconsideration of these published reports gives us confidence that our estimate of

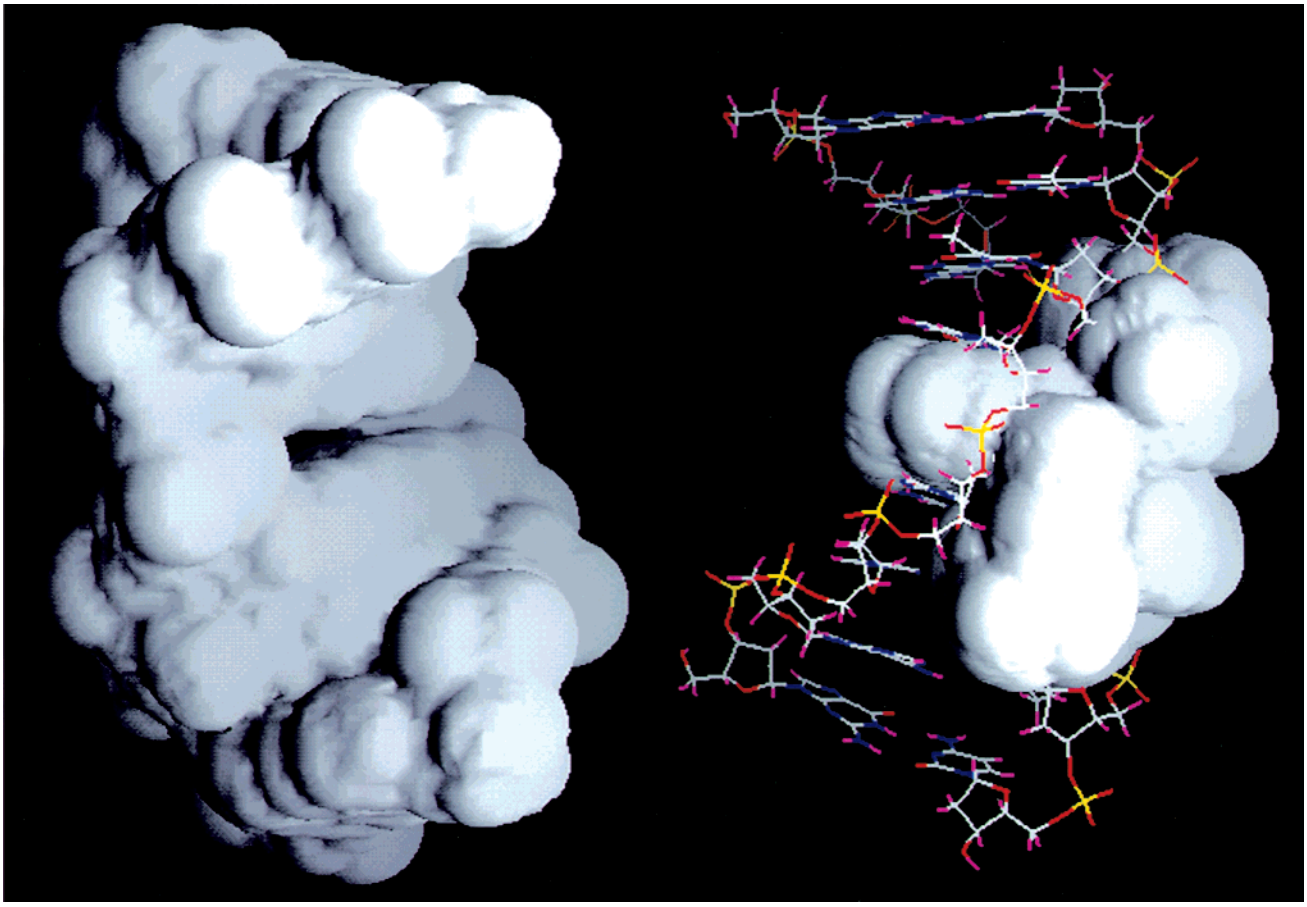

FIGURE 2: Solvent-accessible surfaces for DNA intercalation by actinomycin D. (Left) Surface for the d(GAAG·CTTC)$_2$ duplex looking into the minor groove and showing the central GpC intercalation site. (Right) Component surface for the ligand in the 1:1 complex, showing burial of the intercalated planar chromophore and the snug fit of each cyclic pentapeptide residue in the minor groove. Molecular surfaces were generated using the GRASP 1.3.6 program (*23*) using coordinates taken from ref *25* [PDB entry 2D55 (NDB entry ddh037)].

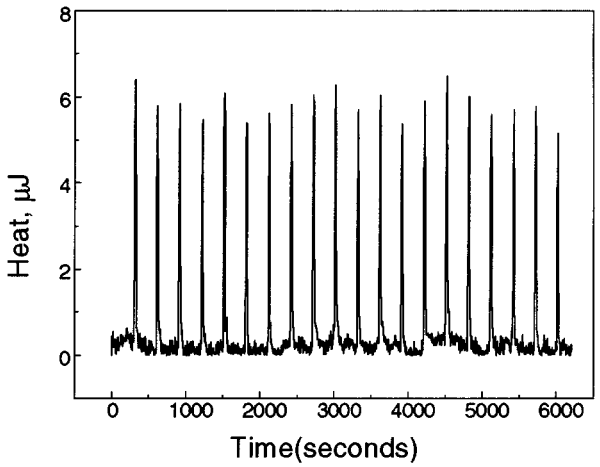

FIGURE 3: Representative primary data from an isothermal titration calorimetry experiment. ITC data at 35 °C are shown for the titration addition of a 1 mM solution of ethidium into 1 mL of calf thymus DNA solution (1 mM in bp) using BPE-S buffer. Serial 3 μL aliquots of ligand solution were added at 5 min intervals.

the heat capacity change for ethidium is both accurate and reliable.

Table 3 shows computed values for the change in the contributions to solvent-accessible surface areas that accompany the DNA binding of the five intercalators that were studied. Changes in the nonpolar surface areas upon binding range from 407 (ethidium) to 1046 Å^2 (actinomycin D). Figure 6 shows that the magnitudes of ΔC_p for intercalators are correlated with the change in nonpolar SASA on binding. Experimental data are also shown for the solvent transfer of small hydrocarbons and for a variety of protein binding and denaturation reactions. The results obtained here for the DNA intercalators nicely fill the wide gap that existed between the two independent and unrelated data sets. Further, our data should be of more general interest to the research community as this represents an additional class of biomolecular reaction for following the predicted links between experimentally accessible thermodynamic parameters (ΔC_p) and otherwise unrelated structural factors.

The Record laboratory (*13*, *31*) previously derived an empirical relationship between ΔC_p and reaction changes in SASA given by $\Delta C_p = 0.32(\pm 0.04)\Delta A_{np} - 0.14(\pm 0.04)\Delta A_p$ cal mol^{-1} K^{-1}, where ΔA_{np} and ΔA_p are the accompanying changes in nonpolar and polar solvent-accessible surface areas (in square angstroms), respectively. If this relationship is used to compute expected ΔC_p values, we obtain the values listed in column 5 of Table 3. Comparison of the calculated and experimental values shows fair agreement, although the experimental ΔC_p values are systematically greater by 13−33%. Another empirical relationship was provided by Murphy and Freire (*12*), use of which yields deviations of 2.5−16% between computed and calculated ΔC_p values, with no systematic trend in the direction of the deviations. It is possible to significantly improve the agreement over both of these by deriving a new relationship using only our DNA binding data for the intercalator systems. Multiple linear

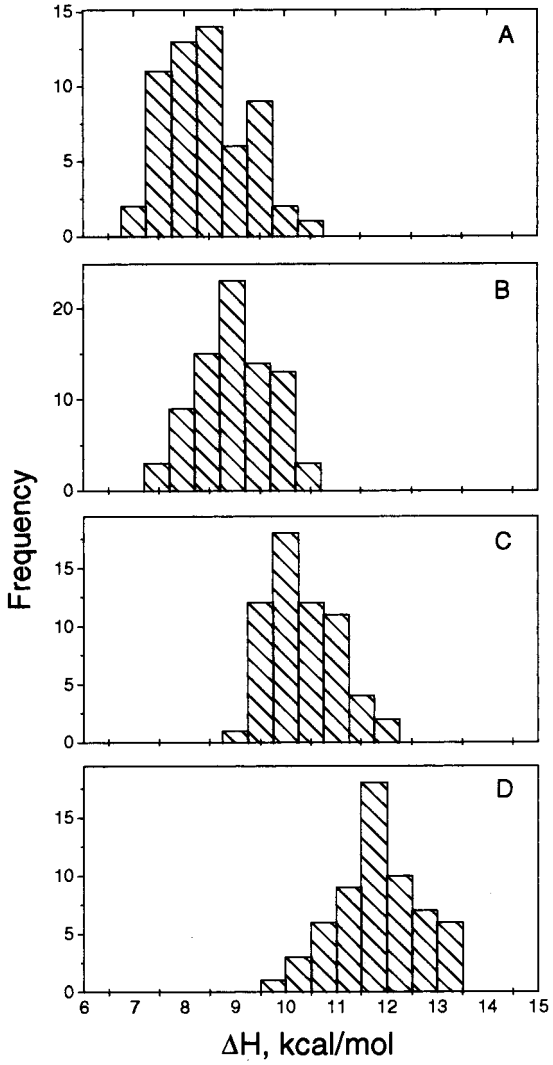

FIGURE 4: Distribution of DNA-binding enthalpy values obtained for ethidium as a function of temperature at (A) 20, (B) 25, (C) 35, and (D) 45 °C. The distributions were obtained from three independent titrations at each temperature, with 20 ligand injections in each ITC experiment.

Table 1: Summary of Measured Enthalpy Values and Calculated Heat Capacity Changes

	ΔH (kcal mol^{-1})[a]				ΔC_p[b] (cal mol^{-1} K^{-1})
compound	20 °C	25 °C	35 °C	45 °C	
ethidium	−8.3 ± 0.9	−9.0 ± 0.8	−10.3 ± 0.7	−11.8 ± 0.8	−139 ± 30
propidium	−6.1 ± 0.7	−6.8 ± 0.8	−8.4 ± 0.8	−9.8 ± 1.2	−150 ± 29
daunorubicin	−9.0 ± 0.8	−9.6 ± 0.9	−11.1 ± 0.9	−13.0 ± 1.2	−160 ± 33
adriamycin	−7.4 ± 0.6	−7.9 ± 0.7	−9.7 ± 1.2	−11.0 ± 1.3	−149 ± 33

[a] Values are the means of 60 determinations at each temperature. The estimated error is the standard deviation of the mean. [b] Heat capacity change calculated from the slope $\delta(\Delta H)/\delta T$ obtained by a weighted linear least-squares fit to the data shown in Figure 5. Data were weighted as $1/(SD)^2$, where SD is the standard deviation. Error estimates were derived by Monte Carlo methods (*26*).

regression using experimental ΔC_p values and the component ΔA_{np} and ΔA_p SASA terms (Table 3) gives the new relationship $\Delta C_p = 0.382(\pm 0.026)\Delta A_{np} - 0.121(\pm 0.077)\Delta A_p$ cal mol^{-1} K^{-1} [$r = 0.995$ ($n = 5$)]. This slight adjustment of the parameter coefficients yields an equation that may be used to compute ΔC_p values in better agreement with the experimental data (column 6 in Table 3), where divergence

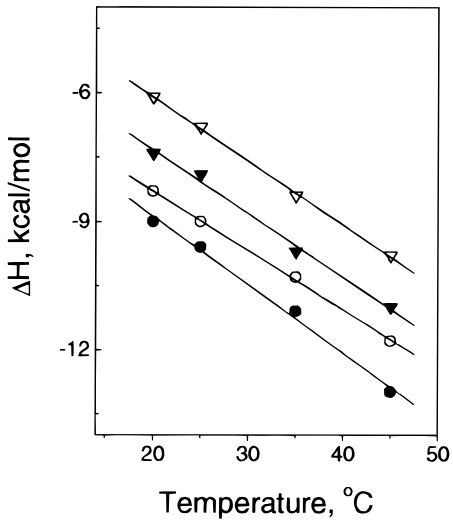

FIGURE 5: Temperature dependence of binding enthalpy (ΔH) values. The solid lines are linear least-squares fits to data for propidium iodide (▽), adriamycin (▼), ethidium (○), and daunorubicin (●).

Table 2: Enthalpy and ΔC_p Values Estimated for the Interaction of Actinomycin D with Oligodeoxynucleotide Duplexes of Defined Sequence[a]

sequence[b]	$\Delta H°$ (10 °C) (kcal mol^{-1})	$\Delta H°$ error[c] (kcal mol^{-1})	ΔC_p (cal mol^{-1} K^{-1})	ΔC_p error[c] (cal mol^{-1} K^{-1})
5′-CTATGCATAT	−2.7	⟨−3.6; −1.8⟩	−364	⟨−473; −255⟩
5′-CTACGCATAT	1.6	⟨1.4; 1.8⟩	−423	⟨−448; −399⟩
5′-CTATGGGTAC	−0.2	⟨−0.4; −0.1⟩	−337	⟨−357; −316⟩
			average $\Delta C_p = -375(\pm 44)$[d]	

[a] Obtained from a reanalysis of the published data of Bailey et al. (*27*), as described in the Supporting Information. [b] Base sequence for one complementary strand of the host DNA duplex. [c] Lower and upper bounds of the confidence interval of the fitted parameters are shown, determined at the 65% level. [d] Mean value ± standard deviation.

is now only 3−9% for the disparate ligands involved. The new empirical relationship also yields better agreement with the experimentally determined ΔC_p value for the DNA minor groove-binding Hoechst 33258 dye (last entry in Table 3). It is important to realize that the values of empirical parameters used to correlate ΔC_p with ΔA_{np} and ΔA_p depend on the algorithm and radii used to compute the changes in solvent-accessible surface areas (*12*). The improved agreement of observed and calculated ΔC_p values with our newly derived relationship most probably arises from subtle differences between our approach and that used by others in the computation of solvent-accessible surface areas.

Knowledge of reliable ΔC_p values provides insight into the hydrophobic contribution to the intercalative DNA binding reactions. Record and colleagues have shown that $\Delta G_{hyd} = 80\Delta C_p$ within about 25% error (*31*). Table 3 shows the calculated hydrophobic contribution to the binding free energy for the intercalators that were studied; ΔG_{hyd} is large and negative in all cases, with values ranging from −11.2 kcal mol^{-1} for ethidium to −30 kcal mol^{-1} for the larger actinomycin D molecule. For comparison, a value of −26.4 kcal mol^{-1} was estimated for the binding of Hoechst 33258 to the DNA minor groove (*7*). The large, negative values of ΔG_{hyd} for DNA intercalators indicate that their binding is driven at least in part by a large favorable contribution from the hydrophobic effect.

Table 3: Summary of Changes in Solvent-Accessible Surface Areas (SASAs), Experimental versus Calculated Heat Capacity Changes, and Hydrophobic Free Energy Terms for the DNA Intercalators Studied, and for the Hoechst 33258 Groove-Binding Dye

compound	$-\Delta A_{np}$[a] (Å^2)	$-\Delta A_{p}$[a] (Å^2)	expt[b] ΔC_p (cal mol^{-1} K^{-1})	calcd[c] ΔC_p (cal mol^{-1} K^{-1})	calcd[d] ΔC_p (cal mol^{-1} K^{-1})	ΔG_{hyd}[e] (kcal mol^{-1})
intercalator						
ethidium	407 (5)	96	−139	−117(±17)	−144(±13)	−11.2
propidium	468[f] (5)	121[f]	−150	−133(±19)	−164(±15)	−12.0
daunorubicin	510 (7)	232	−160	−131(±22)	−167(±22)	−12.8
adriamycin	462 (5)	257	−149	−112(±21)	−145(±23)	−12.0
actinomycin D	1046 (9)	285	−375[g]	−295(±43)	−365(±35)	−30.0
groove binder						
Hoechst 33258[h]	917 (2)	185	−330	−267(±37)	−328(±28)	−26.4

[a] Mean burial of nonpolar (np) or polar (p) SASA per intercalation calculated as described in the text. The number of deposited structures used for analysis is shown in parentheses. [b] Determined by ITC. [c] Calculated from Spolar and Record (*13*) using $\Delta C_p = 0.32(\pm 0.04)\Delta A_{np} - 0.14(\pm 0.04)\Delta A_p$. [d] Calculated using $\Delta C_p = 0.382(\pm 0.026)\Delta A_{np} - 0.121(\pm 0.077)\Delta A_p$, where the coefficients were obtained by linear regression using data for the five intercalators as a basis set. [e] Hydrophobic contribution to the experimental binding free energy, calculated from the linear relationship $\Delta G_{hyd} = 80\Delta C_p$. [f] Models for two low-energy ligand arrangements (i.e., N^+-Me group in the side chain pointing toward or away from the DNA) were averaged for analysis. [g] Obtained from van't Hoff analysis. Average of the three values shown in Table 2. [h] Averaged data for the $d(CGCA_3T_3GCG)_2$−dye complex taken from Haq et al. (*7*, *22*).

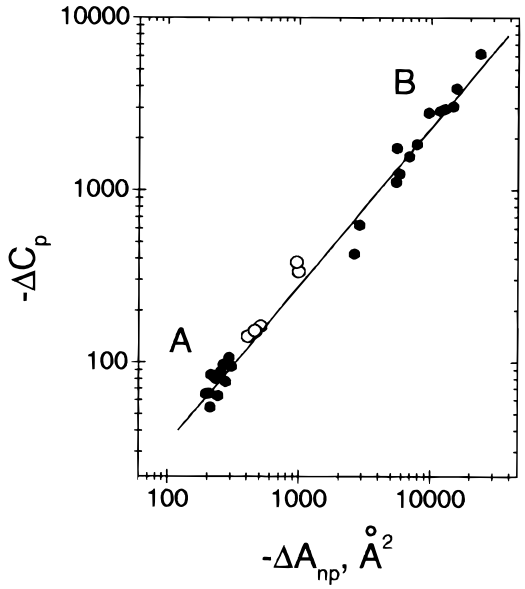

FIGURE 6: Correlation of heat capacity changes and binding-induced burial of nonpolar SASA. Our data for DNA intercalators are shown as open circles. Data shown as solid circles were taken from Livingstone et al. (*28*). Region A represents data for the transfer of small hydrocarbons from water to nonpolar solvents. Region B represents data for protein unfolding and binding reactions.

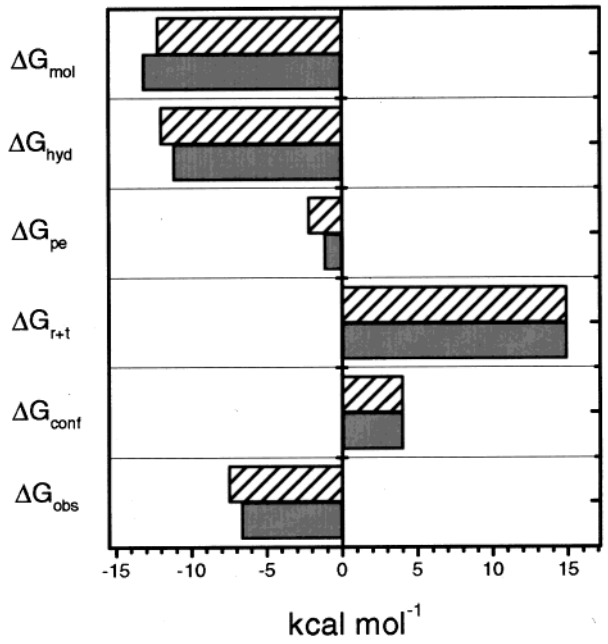

FIGURE 7: Parsing the free energy (ΔG_{obs}) of DNA binding for ethidium (hatched bars) and propidium (gray bars) into the contributor energy terms.

Once a detailed thermodynamic profile is obtained, it is possible to attempt parsing of the observed binding free energy for an intercalation process to reveal the underlying contributions from various molecular interactions (*6*−*9*). The observed binding free energy (ΔG_{obs}) contains contributions from at least five component terms:

$$\Delta G_{obs} = \Delta G_{conf} + \Delta G_{r+t} + \Delta G_{pe} + \Delta G_{hyd} + \Delta G_{mol}$$

In this equation, ΔG_{conf} is the contribution from conformational transitions in the DNA and intercalator, ΔG_{r+t} is the free energy cost for the restriction of rotational and translational freedom, ΔG_{pe} is the polyelectrolyte contribution, ΔG_{hyd} is the hydrophobic contribution, and ΔG_{mol} is the contribution of all other molecular interactions (e.g., van der Waals interactions, H-bonding, etc.). A detailed discussion of the contributor terms and their magnitudes has been published elsewhere (*6*).

We will attempt to parse the binding free energies obtained for ethidium and propidium into the component terms. Figure 7 shows our best estimates for each of the free energy contributions. Binding free energies (ΔG_{obs}) of −6.7 and −7.5 kcal mol^{-1} were determined for ethidium and propidium, respectively, at 25 °C in buffer containing 0.2 M NaCl (*6*, *9*). Since there is no evidence to suggest that either ethidium or propidium significantly changes conformation upon intercalation, the only contribution to ΔG_{conf} arises from the energetic cost of deforming DNA to generate an intercalation site. The best estimate for this free energy contribution stems from the kinetic studies of MacGregor and co-workers (*32*), who observed a conformational transition in DNA that preceded ethidium binding that was interpreted as an opening of the stacked base pairs. A free energy of 4.0 kcal mol^{-1} characterized the conformational transition, which we will assign to ΔG_{conf} for both ethidium and propidium. For a rigid-body association, ΔG_{r+t} is approximately 15 kcal mol^{-1}, a value that is subject to some

debate but which we believe is most applicable for intercalation reactions (*6*). From the salt dependence of binding constants, ΔG_{pe} was estimated to be -1.2 and -2.2 kcal mol^{-1} for ethidium and propidium, respectively, in 0.2 M NaCl (*9*). Values of ΔG_{hyd} were calculated (Table 3) using the empirical relationship (*31*) outlined above. Assigning a value to ΔG_{mol} is the most problematic task of the parsing exercise. Our approach is to sum the four contributions discussed up to this point, and to then subtract this value from ΔG_{obs}. This yields estimates for ΔG_{mol} of approximately -13 kcal mol^{-1} for intercalation by ethidium or propidium. Best estimates for the contributions to the observed free energies for these two ligands are shown in Figure 7. The picture that emerges from this analysis of energetics for the binding reactions of these intercalators is that the process is a delicate balance between opposing forces. The energetic cost of forming an intercalation site and the general cost of restricting both the translational and rotational freedom of the ligand oppose the reaction. Favorable polyelectrolyte and hydrophobic contributions balance these unfavorable free energy terms, but additional free energy contributions from other molecular interactions are needed to account for the observed binding free energy.

Does the estimate for ΔG_{mol} of approximately -13 kcal mol^{-1} for ethidium and propidium intercalation make sense? We believe it does, and rationalize the magnitude of this contribution as follows. In contrast to more elaborate intercalating molecules such as daunorubicin and actinomycin D, neither ethidium nor propidium has substituents that are likely to hydrogen bond to DNA within the intercalated complex. The molecular interactions most likely to occur will involve van der Waals contacts, primarily between the intercalated phenanthridine ring and base pairs that comprise the immediate intercalation site. Makhatadze and Privalov (*11*) estimate that van der Waals contact between aromatic surfaces yields a favorable free energy of -42 cal mol^{-1} Å^{-2}. If we assume this factor, then -13 kcal mol^{-1} of free energy could be obtained if 310 Å^2 of ethidium or propidium surface were in bound contact with the DNA molecule, an entirely reasonable value. As the total solvent-accessible surface areas (Table 3) for ethidium and propidium are 503 and 589 Å^2, respectively, this implies that only 50−65% of each ligand would need to be in van der Waals contact with the host DNA duplex.

We caution that the above parsing exercise is both tentative and approximate. Values for at least some of the free energy terms are in fact controversial and subject to debate. A detailed and balanced discussion of each free energy term was presented in ref *6*, along with a rationalization for the selection of the particular values used above. The appropriate value of ΔG_{r+t} to use is especially controversial, and at least one recent publication (*40*) suggests that a value 2−3 times lower than what we have assumed is in fact to be preferred. In that study (*40*), the estimate for ΔG_{r+t} was obtained from careful differential scanning calorimetry experiments that compared the denaturation of a native dimeric protein with that of a construct in which the two polypeptides were linked by a single cross-link. While the measurements were as precise as possible, the value ΔG_{r+t} that was obtained was the result of a comparatively small difference between two large numbers, and is also subject to assumptions concerning the contributions of vibrational modes to the rotational and translational entropy of the native and constructed proteins.

The magnitudes of the values we chose for ΔG_{r+t} and ΔG_{conf} are (as one astute reviewer pointed out) probably upper limits, and values of the lower magnitude could arguably be used. If that were done, the effect would be to increase the magnitude of the contribution of ΔG_{mol} to be accounted for. Despite the tentative nature of the parsing exercise, it remains valuable and provides insight into the intercalation process, as long as its current limitations are recognized.

The free energy contributions to these intercalation reactions provide interesting contrasts to the binding energetics of the DNA minor groove binder Hoechst 33258 described in previous work from our laboratories (*7*, *22*). For each binding process, favorable free energy contributions are found to come from polyelectrolyte and hydrophobic free energy terms, although the latter contribution is much larger for the Hoechst dye than for either ethidium or propidium. While intercalative binding involves an unfavorable penalty in terms of the free energy required to form an intercalation site, the DNA structure is essentially unperturbed upon groove binding (i.e., $\Delta G_{conf} = 0$ for the DNA−dye complex). The most interesting contrast involves the ΔG_{mol} term. A small *positive* value for ΔG_{mol} was inferred for interaction with the Hoechst 33258 ligand, whereas a large, negative value is required for ethidium and propidium to match the observed binding free energy. Hoechst 33258 binding was found to be driven primarily by hydrophobic interactions, whereas ethidium binding and propidium binding are driven almost equally by hydrophobic forces and other intermolecular contacts within the intercalation site. We contend that the latter terms chiefly stem from van der Waals interactions between the host DNA and the bound intercalator molecule.

SUMMARY AND CONCLUSIONS

Our results show that DNA−ligand intercalation reactions are accompanied by heat capacity changes that are comparatively small in magnitude but which are nonetheless significant. The measured ΔC_p values and their associated errors should serve to clarify previous contradictory reports in the literature concerning the magnitudes and even the existence of heat capacity changes for such binding processes.

These results should have significant impact upon the design of new DNA-targeted molecules that involve an intercalative mode of binding to the host molecule. It is now emerging that molecular design methods can be used to effectively "tailor" an intercalator molecule for structure-selective recognition of a DNA biotarget, with examples now identified for duplex (e.g., refs *4* and *33*), triplex (*34*), and tetraplex (*35*, *36*) DNA systems. For the first time, the availability of an equation that can directly link an experimentally accessible thermodynamic parameter (ΔC_p) and structural factors enables a rapid assessment of optimal characteristics for a candidate drug or ligand molecule. Particular features can be incorporated to enhance or modulate the burial of surface area from each reactant, especially nonpolar molecular surface, so as to direct the binding behavior. Our analysis of the free energy contributions that drive DNA intercalation suggests that the design process requires a greater focus on molecular features that

optimize or promote the removal of hydrophobic solvent-accessible surfaces and increase van der Waals contacts.

ACKNOWLEDGMENT

We thank Dr. David E. Graves (University of Mississippi, Jackson, MS) for helpful discussions concerning his actinomycin D binding data.

NOTE ADDED IN PROOF

Dr. W. David Wilson (Georgia State University) has provided us with a preprint of an article entitled "Thermodynamic and Structural Analysis of DNA Minor Groove Complex Formation" that has been accepted for publication in the *Journal of Molecular Biology*. In that study, ΔC_p values were determined for the DNA groove binding of three diphenylfuran dications. ΔC_p values were found to correlate well with computed changes in solvent-accessible surface areas. The results we report here for intercalators and those described for the diphenylfurans are mutually consistent and complementary.

SUPPORTING INFORMATION AVAILABLE

Further details relating to the determination of ΔC_p values for DNA intercalation by actinomycin D, a reanalysis of published van't Hoff data for ethidium binding, and the calculation of solvent-accessible surface areas for the intercalator complexes (two figures and six tables). This material is available free of charge via the Internet at http://pubs.acs.org.

REFERENCES

1. Chaires, J. B. (1998) *Curr. Opin. Struct. Biol. 8*, 314−320.
2. Wemmer, D. E., and Dervan, P. B. (1997) *Curr. Opin. Struct. Biol. 7*, 355−361.
3. Thurston, D. E. (1999) *Br. J. Cancer 80* (Suppl. 1), 65−85.
4. Jenkins, T. C. (2000) *Curr. Med. Chem. 7*, 99−115.
5. Mergny, J. L., and Hélène, C. (1998) *Nat. Med. 4*, 1366−1367.
6. Chaires, J. B. (1997) *Biopolymers 44*, 201−215.
7. Haq, I., Ladbury, J. E., Chowdhry, B. Z., Jenkins, T. C., and Chaires, J. B. (1997) *J. Mol. Biol. 271*, 244−257.
8. Chaires, J. B., Satyanarayana, S., Suh, D., Fokt, I., Przewloka, T., and Priebe, W. (1996) *Biochemistry 35*, 2047−2053.
9. Chaires, J. B. (1996) *Anti-Cancer Drug Des. 11*, 569−580.
10. Sturtevant, J. M. (1977) *Proc. Natl. Acad. Sci. U.S.A. 74*, 2236−2240.
11. Makhatadze, G. I., and Privalov, P. L. (1995) *Adv. Protein Chem. 47*, 307−425.
12. Murphy, K. P., and Freire, E. (1995) *Pharm. Biotechnol. 7*, 219−241.
13. Spolar, R. S., and Record, M. T., Jr. (1994) *Science 263*, 777−784.
14. Neidle, S. (1997) *Bioplolymers 44*, 105−121.
15. Hopkins, H. P., Jr., Fumero, J., and Wilson, W. D. (1990) *Biopolymers 29*, 449−459.
16. Taquet, A., Labarbe, R., and Houssier, C. (1998) *Biochemistry 37*, 9119−9126.
17. Chaires, J. B. (1997) *Biophys. Chem. 64*, 15−23.
18. Jenkins, T. C. (1997) in *Methods in Molecular Biology, Vol. 90: Drug−DNA Interaction Protocols* (Fox, K. R., Ed.) Chapter 14, pp 195−218, Humana Press, Totawa, NJ.
19. Chaires, J. B., Dattagupta, N., and Crothers, D. M. (1982) *Biochemistry 21*, 3933−3940.
20. Grenthe, I., Ots, H., and Ginstrup, O. (1970) *Acta Chem. Scand. 24*, 1067−1080.
21. Haq, I. (1998) in *Biocalorimetry: Applications of Calorimetry in the Biological Sciences* (Ladbury, J. E., and Chowdhry, B. Z., Eds.) pp 81−93, John Wiley & Sons, Chichester, U.K.
22. Haq, I., Jenkins, T. C., Chowdhry, B. Z., Ren, J., and Chaires, J. B. (2000) in *Methods in Enzymology, Volume 323: Energetics of Biological Macromolecules* (Ackers, G., and Johnson, M. L., Eds.) Academic Press, San Diego, CA. (in press).
23. Nicholls, A., Sharp, K., and Honig, B. (1991) *Proteins: Struct., Funct., Genet. 11*, 281−296 (GRASP program available from: http://trantor.bioc.columbia.edu/grasp).
24. Berman, H. M., Olson, W. K., Beveridge, D. L., Westbrook, J., Gelbin, A., Demeny, T., Hsieh, S. H., Srinivasan, A. R., and Schneider, B. (1992) *Biophys. J. 63*, 751−759.
25. Shinomiya, M., Chu, W., Carlson, R. G., Weaver, R. F., and Takusagawa, F. (1995) *Biochemistry 34*, 8481−8491.
26. Straume, M., and Johnson, M. L. (1992) in *Methods in Enzymology 210: Numerical Computer Methods* (Brand, L., and Johnson, M. L., Eds.) pp 117−129, Academic Press, San Diego, CA.
27. Bailey, S. A., Graves, D. E., Rill, R., and Marsch, G. (1993) *Biochemistry 32*, 5881−5887.
28. Livingstone, J. R., Spolar, R. S., and Record, M. T., Jr. (1991) *Biochemistry 30*, 4237−4244.
29. Baldini, G., and Varani, G. (1986) *Biopolymers 25*, 2187−2208.
30. Sauer, B. B., Flint, R. A., Justice, J. B., and Trowbridge, C. G. (1984) *Arch. Biochem. Biophys. 234*, 580−584.
31. Record, M. T., Jr., Ha, J.-H., and Fisher, M. A. (1991) *Methods Enzymol. 208*, 291−344.
32. Macgregor, R. B., Jr., Clegg, R. M., and Jovin, T. M. (1987) *Biochemistry 26*, 4008−4016.
33. Jenkins, T. C. (1997) *DNA Template-Directed Drug Design: Old Toys, New Methods and a Fresh Approach*, Greenwich University Press, London.
34. Haq, I., Ladbury, J. E., Chowdhry, B. Z., and Jenkins, T. C. (1996) *J. Am. Chem. Soc. 118*, 10693−10701.
35. Haq, I., Trent, J. O., Chowdhry, B. Z., and Jenkins, T. C. (1999) *J. Am. Chem. Soc. 121*, 1768−1779.
36. Perry, P. J., and Jenkins, T. C. (1999) *Expert Opin. Invest. Drugs 8*, 1981−2008.
37. Thomas, G., and Roques, B. (1972) *FEBS Lett. 26*, 169−175.
38. Bresloff, J. L. (1974) Ph.D. Thesis, Yale University, University Microfilms International, Ann Arbor, MI, pp 65−74.
39. Chaires, J. B., Dattagupta, N., and Crothers, D. M. (1982) *Biochemistry 21*, 3927−3932.
40. Tamura, A., and Privalov, P. L. (1997) *J. Mol. Biol. 273*, 1048−1060.

BI000474A